JOURNAL OF MATERIALS SCIENCE 30 (1995) 509–513

Multiple cracking of a coating layer and its influence on fibre strength

Part II *Monte Carlo simulation*

S. OCHIAI, M. HOJO
Mesoscopic Materials Research Centre, Faculty of Engineering, Kyoto University, Kyoto 606, Japan

Multiple cracking of a coating layer and its influence on the tensile strength of the coated fibre in the case of strong interfacial bonding were simulated by means of a Monte Carlo method. Within the range where the coating layer was weak, it was found that the weaker the coating layer, the larger became the number of cracks and consequently the smaller became the crack spacing, resulting in higher strength of the fibre. When the strength of the layer was high, however, the crack spacing became large, resulting in a low strength of the fibre comparable to the strength for the case of single cracking. The strength value of the fibre calculated for average crack spacing gave an upper bound, and that calculated for single cracking a lower bound, for the actual fibre strength.

1. Introduction

When coated fibres are pulled in tension, the coating layer sometimes shows multiple cracking, which reduces fibre strength when the interfacial bonding is strong. In this multiple cracking process, the number of cracks and crack spacing vary with varying applied stress. Furthermore, these variations differ from sample to sample. In order to describe the influence of the multiple cracking on fibre strength, a method is required to identify the strength-determining crack of all the cracks and also a method to describe probabilistic affairs such as crack spacing, location of cracks and the difference in cracking behaviour of the samples. In Part I [1], a method to calculate the energy release rates of the fibre at formed cracks for non-uniform crack spacing was presented, with which the strength-determining crack can be identified. In the present paper, the latter method will be presented based on the Monte Carlo simulation technique, because it is known that the application of this technique can describe well the multiple fracture of a tungsten fibre embedded in a copper matrix composite [2] and that of 90° ply in a 0°/90°/0° type graphite/epoxy laminate composite [3]. Using this technique in combination with the calculation method presented in Part I [1], the multiple cracking behaviour of the coating layer and the strength of the fibre will be simulated.

2. Monte Carlo simulation

The Monte Carlo simulation was carried out following the flow chart shown in Fig. 1. The details of the procedure are as follows.

(a) The coating layer with an initial length L_f (= length of fibre) was divided into a large number of N_e elements with a length, L_e, as shown in Fig. 2a.

(b) The strength of the coating layer was assumed to obey the two-parameter Weibull distribution [4]. This distribution function provides the probability, F, of failure at stress, σ, as

$$F = 1 - \exp[-(V/V_0)(\sigma/\sigma_0)^w] \quad (1)$$

where w and σ_0 are the shape and scale parameters, respectively, and V and V_0 are the volume of the material and the standard volume, respectively. The strength (σ in Equation 1) of each coating-layer element was determined by generating a random value, which was substituted for F in Equation 1, together with the values of w, σ_0, V_0 and the volume of each element $V = \pi[(R_f + a)^2 - R_f^2]L_e$, where R_f and a are the radius of the fibre and the thickness of the coating layer, respectively. With the repetition of this process, the strength of element 'r', $S(r)$, was determined for $r = 1$–N_e.

(c) Given the applied net stress on the fibre, σ_f, broken coating-layer elements with $S(r) = 0$ were searched for and the length of each segment of the coating layer (= crack spacing) was obtained. Then the stress exerted in each element was calculated using the method shown in Part I [1]. In the simulation, the exerted stress at the mid-point along the tensile axis of each coating-layer element was, to a first approximation, taken as the representative stress of element 'r', $\sigma_c(r)$; namely, as shown in Fig. 2b, the stress distributions in segments shown with solid curves were approximated to those shown by broken lines. In this process, as the stress in the coating layer varies with varying radial distance, the stress averaged along the

0022–2461

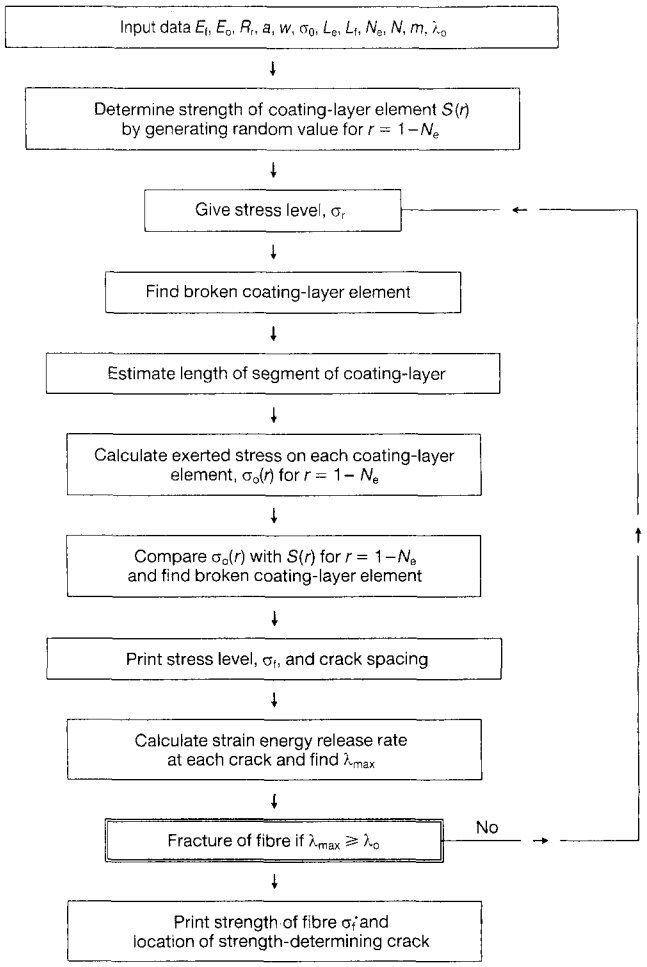

Figure 1 The flow chart of the present Monte Carlo simulation.

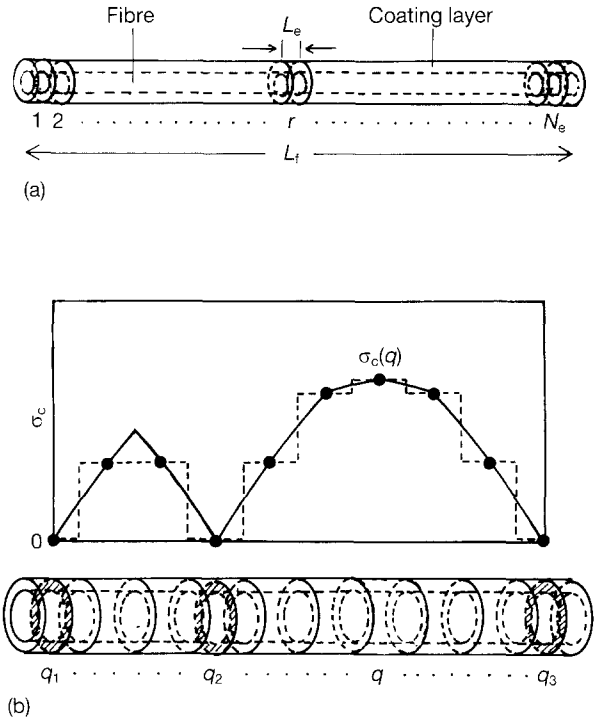

Figure 2 (a) Schematic representation of coating-layer elements with a length L_e and (b) the exerted stress, σ_c, on each element, where elements q_1, q_2, and q_3 have been broken already. The solid curves show the stress distributions in the segments of the coating layer, which are approximated by the broken lines in the simulation.

radial direction was used as the stress exerted on the coating layer.

(d) Whether or not fracture of element 'r' occurs was judged by comparing the stress $\sigma_c(r)$ with the strength $S(r)$: if $\sigma_c(r)$ was higher than $S(r)$, fracture of the element was judged to occur. When the fracture of the element r occurred, $S(r)$ was set to zero. For instance, when elements q_1, q_2 and q_3 had been broken at a given stress level (namely $S(q_1) = S(q_2) = S(q_3) = 0$) as shown in Fig. 2b, if the stress on element q, $\sigma_c(q)$, was higher than the strength $S(q)$, element q was judged to be broken. $S(q)$ was set to zero at this stress level.

(e) At each applied stress level, the locations of cracks (broken coating-layer elements) were searched for. Using the calculation method presented in our Part I [1], the energy release rate of the fibre, λ, was calculated for each crack. The highest energy release rate of all the cracks, λ_{max}, was searched for and compared with the critical energy release rate of the fibre λ_c. When $\lambda_{max} \geq \lambda_c$, the fibre was judged to be broken.

(f) The stress level was raised in steps of 0.5 MPa from zero until the fracture of the fibre occurred. At each stress level, procedures (c–e) were repeated.

In the present work, the following values were used as an example. Radius of the fibre $R_f = 4$ μm; thickness of the coating layer $a = 0.05$–0.5 μm; Young's moduli of the fibre and coating layer, $E_f = 200$ and $E_c = 400$ GPa, respectively; the length of each element $L_e = 0.05$ μm; the length of the fibre $L_f = 100$ μm; the number of elements of the coating layer $N_e = 2000$; the shape and scale parameters of the Weibull distribution $w = 5$ and $\sigma_0 = 50$–500 MPa, respectively; and the standard volume in the Weibull distribution function $V_0 = 1\ mm^3$. The G_f and G_c values were calculated from $G = E/[2(1 + \nu)]$ in which the values ν for the fibre and coating layer were taken to be 0.3. The critical energy release rate of the fibre, λ_c, was taken to be $3\ J\,m^{-2}$, and the fibre stress at $\lambda_{max} = \lambda_c$ was defined as σ_f^*.

Within the present framework, L_f value was taken to be small (100 μm) in comparison with the usual gauge length for the tensile test of the fibre, because the strength of the longer fibre can be determined in a similar manner, and also it can be obtained from the simulation results for a short fibre when the weakest-link reasoning is applied; for instance, if the fibre is 1000 times longer than the simulated fibre, the lowest strength value of the 1000 simulated fibres gives the strength.

In the simulation, the applied stress was raised until the fibre was broken by the crack formed by the fracture of the coating layer, and the σ_f^* value corresponding to crack propagation was obtained. This σ_f^* value is, however, not necessarily equal to the strength value, because the strength of a coated fibre, whose interfacial bonding strength is high enough to prevent debonding and coating-layer fracture prior to that of the fibre, is determined by the sequence between σ_f^* and the strength of the bare fibre, σ_{fu}^o; if $\sigma_f^* > \sigma_{fu}^o$, the fibre is not broken by the crack formed but by its intrinsic defects, so that the fibre strength is given by

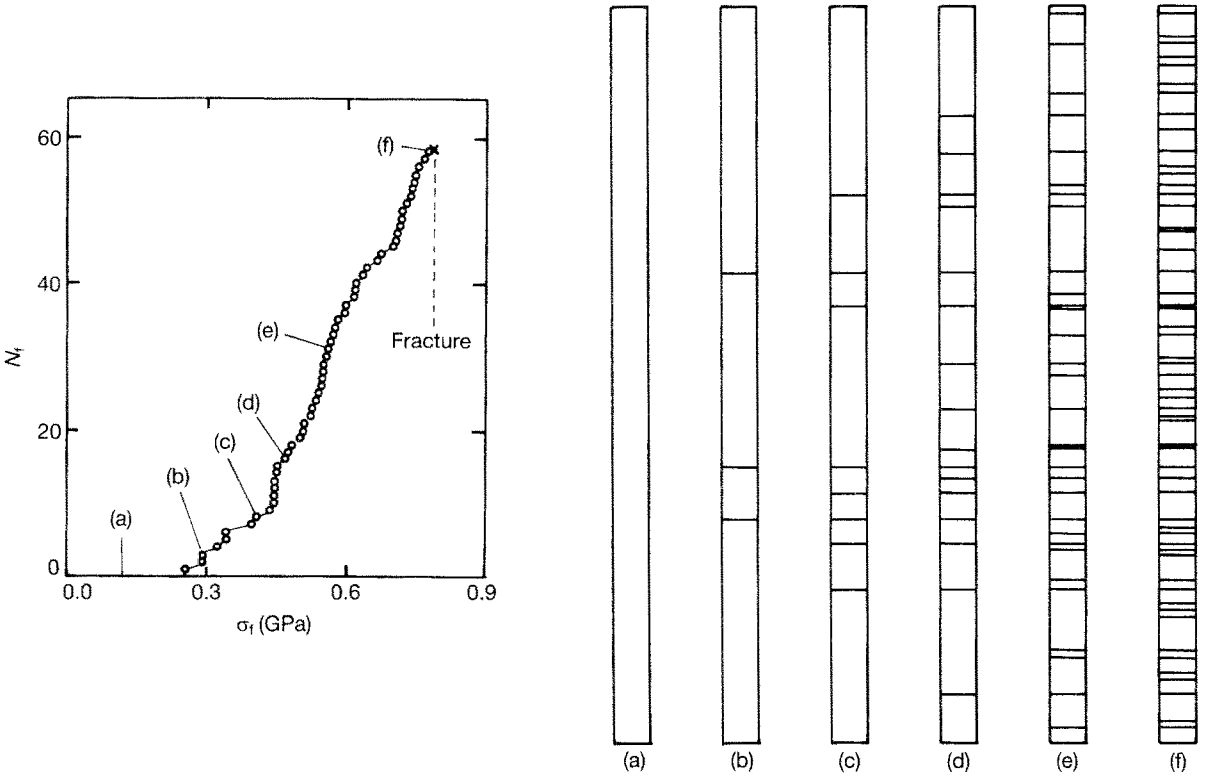

Figure 3 An example of multiple cracking behaviour of the coating layer for $\sigma_0 = 250$ MPa and $a = 0.2$ μm. The variation of N_f as a function of σ_f is shown on the left, and the morphologies of the cracked coating layer at (a–f) are shown on the right.

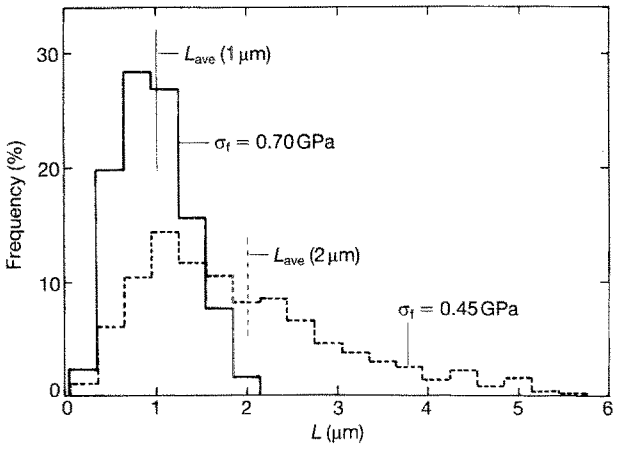

Figure 4 Examples of the distribution of the length of segments at $\sigma_f = 0.45$ and 0.70 GPa for $\sigma_0 = 150$ MPa and $a = 0.2$ μm. The average lengths were nearly 2 and 1 μm at $\sigma_f = 0.45$ and 0.70 GPa, respectively.

σ_{fu}°, while if $\sigma_f^* < \sigma_{fu}^{\circ}$, the fibre is broken by the crack formed so that the fibre strength is given by σ_f^* [5]. In this work, the results for the case where $\sigma_f^* < \sigma_{fu}^{\circ}$ will be given in Section 3.2 and those for both $\sigma_f^* < \sigma_{fu}^{\circ}$ and $\sigma_f^* > \sigma_{fu}^{\circ}$ in Section 3.3.

3. Results and discussion

3.1. Crack spacing

Fig. 3 shows an example of the simulation results for $a = 0.2$ μm and $\sigma_0 = 250$ MPa. In this example, $\sigma_0 = 250$ MPa corresponds to the average strength, 420 MPa, for the coating layer with the present gauge length. The number of fractures, N_f, is plotted against applied stress, σ_f. The initially continuous coating layer was broken continually into shorter segments. The morphologies of the coating layer varied from (a) where no cracking occurred, to (f) where the fibre was broken. The stress levels for (a–f) are indicated in the N_f–σ_f curve. As shown in (b–f), the crack spacing is not uniform.

Fig. 4 shows the distribution of the crack spacing at $\sigma_f = 0.45$ and 0.70 GPa for $\sigma_0 = 150$ MPa. The average crack spacings, L_{ave}, were nearly 2 and 1 μm at $\sigma_f = 0.45$ and 0.70 GPa, respectively. Fig. 4 indicates that the crack spacing is widely scattered in the multiple cracking process. Fig. 5 shows the difference in cracking behaviour of three samples for $a = 0.2$ μm and $\sigma_0 = 150$ MPa. Each sample behaves differently. As shown in Figs 3–5, the number of cracks and crack spacing vary with varying applied stress level and also from sample to sample. The fibre strength is affected by these probabilistic factors.

3.2. Influence of the strength of the coating layer on fibre strength

The average strength of the coating layer increases with increasing σ_0. The influence of the strength of the coating layer for $a = 0.2$ μm was simulated by changing the value of σ_0. In this case, the average strengths of the coating layer with the initial length are, for instance, 83, 167, 500 and 833 MPa for $\sigma_0 = 50$, 100, 300 and 500 MPa, respectively, while the coefficient of variation of strength of the coating layer is 22.9% for all values of σ_0, because the w is fixed at 5.

Fig. 6 shows typical morphologies of the cracked coating layer at the fracture of fibres and the locations of strength-determining cracks as indicated by arrows. In this example, (a–c) correspond to $\sigma_0 = 150$, 300

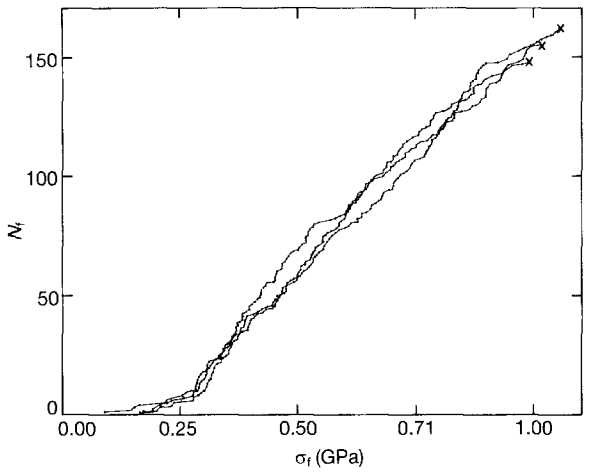

Figure 5 Examples of the variations of N_f with increasing σ_f for three simulations for $\sigma_0 = 150$ MPa and $a = 0.2$ μm: (×) indicates the fracture of fibres.

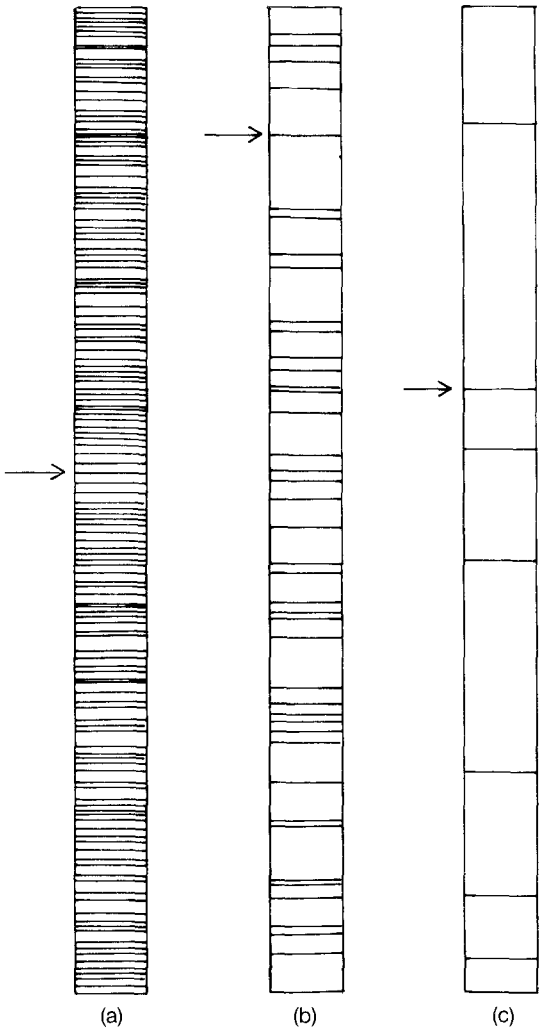

Figure 6 Typical morphologies of the cracked coating layer at the fracture of fibres for $a = 0.2$ μm and $\sigma_0 =$ (a) 150, (b) 300 and (c) 500 MPa. The arrows show the strength-determining cracks.

and 500 MPa, respectively. It is clearly shown that the crack between long segments tends to act as the strength-determining one.

Fig. 7 shows the typical variations of N_f as a function of σ_f for various σ_0 values. Evidently, the lower the strength of the coating layer, the larger

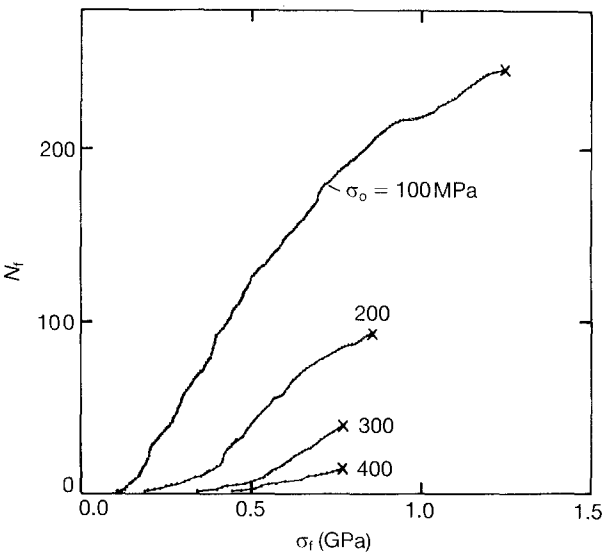

Figure 7 Typical variations of N_f as a function of σ_f for various σ_0 values for $a = 0.2$ μm.

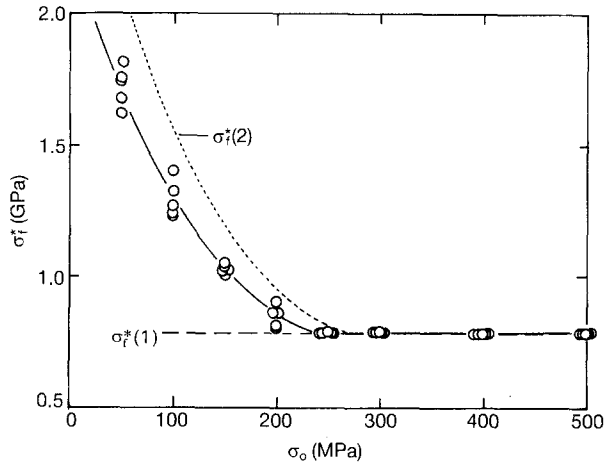

Figure 8 Variation of σ_f^* as a function of σ_0 for $a = 0.2$ μm. The broken and dotted curves show the variations of σ_f^* (1) and σ_f^* (2) for comparison.

became the number of cracks and consequently the smaller became the crack spacing at any σ_f. As a result, the fracture stress of the fibre (×) increased with decreasing σ_0.

Fig. 8 shows the influence of the strength of the coating layer on the fibre strength. Simulation experiments were carried out five times for each σ_0 value. Under the present conditions, the obtained σ_f^* values were lower than 2 GPa. Therefore, if σ_{fu}^o is higher than 2 GPa, the obtained σ_f^* values are equal to the fibre strength because $\sigma_f^* < \sigma_{fu}^o$. The fibre strength for such a case is discussed here. For $\sigma_0 < 300$ MPa, σ_f^* increased with decreasing σ_0, owing to the decrease in crack spacing. On the other hand, for $\sigma_0 > 300$ MPa, the strength values remained nearly constant. This result arises from the large crack spacing, and is explained as follows: the fibre strength for a single crack (only one crack occurs in the coating layer), σ_f^* (1), corresponding to infinite crack spacing, was calculated for comparison. The result is superimposed as the broken line in Fig. 8. At large σ_0 (> 300 MPa), the strength values obtained

by the simulation were comparable with the σ_f^* (1) values. Thus, although multiple cracking also occurs for $\sigma_0 > 300$ MPa (Figs 6 and 7), the strength-determining crack, which essentially exists between longer segments, acts similar to a single crack. In this way, when the coating layer is strong and therefore the crack spacing is large, the fibre strength falls to the level for a single crack in spite of the multiple cracking.

From the simulation, the number of fractures, N_f, was monitored as a function of σ_f. Then using the average crack spacing, L_{ave}, the fibre strength expected from average spacing, σ_f^* (2), was calculated at each σ_0 value. The result is superimposed as the dotted curve, also in Fig. 8. When σ_0 was high (> 300 MPa), σ_f^* (2) was the same as σ_f^* (1) and also the same as the strength values obtained by the simulation. On the other hand, when σ_0 was low (< 300 MPa), the strength values obtained by the simulation were within the range between σ_f^* (1) and σ_f^* (2). Namely, σ_f^* (1) gave a lower bound and σ_f^* (2) an upper bound for fibre strength, while the discrepancy between σ_f^* and σ_f^* (1) was large for low σ_0.

3.3. Influence of thickness of the coating layer on fibre strength

Fig. 9 shows the variation of σ_f^* as a function of the thickness of the coating layer, a, for $\sigma_0 = 100$ and 300 MPa. The broken and dotted curves show the relation of σ_f^* (1) to a for $\sigma_0 = 100$ and 300 MPa and that of σ_f^* (2) to a for $\sigma_0 = 100$ MPa, respectively. For $\sigma_0 = 300$ MPa, the σ_f^* values obtained by the simulation were nearly the same as σ_f^* (1) values for any a, owing to the large crack spacing. On the other hand, for $\sigma_0 = 100$ MPa, the simulation values were within the range between the lower bound of σ_f^* (1) and the upper bound of σ_f^* (2).

When the strength of the bare fibre, σ_{fu}^o (taken to be constant for simplicity), is given, the strength of the coated fibre is described from the sequence between σ_f^* and σ_{fu}^o as stated above. Taking the case of $\sigma_0 = 100$ MPa in Fig. 9 as an example, when σ_{fu}^o is 2 GPa, the fibre strength is given by σ_{fu}^o for the range of $a < a_{crit}$ due to $\sigma_f^* > \sigma_{fu}^o$, but it is given by σ_f^* for $a > a_{crit}$ due to $\sigma_f^* > \sigma_{fu}^o$, where a_{crit} is the critical thickness below which the fibre strength is not reduced by the formed crack, satisfying $\sigma_{fu}^o = \sigma_f^*$. However, as known from Fig. 9, the σ_f^* values vary from sample to sample, suggesting that a_{crit} also varies. To a first approximation, when average σ_f^* values are used, a_{crit} can roughly be estimated to be 0.07 μm. The average fibre strength varies along ABC as a function of a as shown with the solid curve, where B corresponds to $a = 0.07$ μm. In this example, the fibre strength for $a = 0.05$ μm is given by 2 GPa although the σ_f^* values exceed 2 GPa.

If σ_{fu}^o is taken to be more than 2.5 GPa, fibre strength for $a = 0.05$ μm is also given by the simulated σ_f^* value due to $\sigma_f^* < \sigma_{fu}^o$. In such a case, a_{crit} decreases with increasing σ_{fu}^o. In this way, the variation of average strength of the coated fibre can be predicted in a similar procedure to that for any strength of a bare fibre.

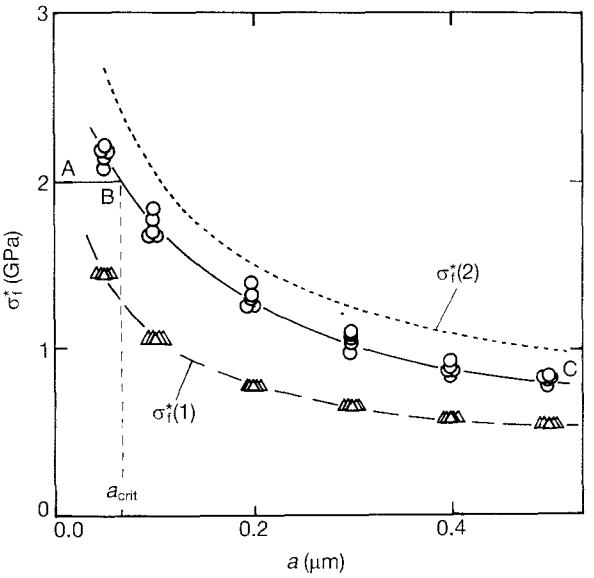

Figure 9 Variations of σ_f^* as a function of a for $\sigma_0 = (\bigcirc)$ 100 and $(\triangle)$ 300 MPa. The broken and dotted curves show the variations of σ_f^* (1) for $\sigma_0 = 100$ and 300 MPa and σ_f^* (2) for $\sigma_0 = 100$ MPa, respectively. If σ_{fu}^o is taken to be 2 GPa, the average strength of the fibre for $\sigma_0 = 100$ MPa varies along ABC as shown by the solid curve.

4. Conclusion

Multiple cracking behaviour of the coating layer and its influence on fibre strength were simulated by a Monte Carlo method. It was demonstrated that the fibre strength can be raised by progressive multiple cracking, in comparison with that for single cracking. Fibre strength increases with decreasing strength of the coating layer when the strength of the coating layer is not high, but becomes low comparable to the strength for a single crack, even though multiple cracking occurs, when the strength of the coating layer is high. The strength of the fibre calculated for average crack spacing gives an upper bound and that calculated for single cracking a lower bound, for the actual fibre strength.

Acknowledgement

The authors thank The Ministry of Education, Science and Culture of Japan for a grant-in-aid (04650649).

References

1. S. OCHIAI and K. HOJO *J. Mater, Sci.* **29** (1994).
2. S. OCHIAI and K. OSAMURA, *Z. Metallkde.* **77** (1986) 249.
3. S. OCHIAI, P. W. M. PETERS and K. SCHULTE, *J. Mater. Sci.* **26** (1991) 5433.
4. W. WEIBULL, *J. Appl. Mech.* **18** (1951) 293.
5. S. OCHIAI and K. OSAMURA, *Met. Trans.* **18A** (1987) 673.

Received 18 March 1993
and accepted 9 June 1994